FULL PAPER

Dalton
www.rsc.org/dalton

Palladium(II) allyl complexes of chiral diphosphazane ligands: ambident coordination behaviour and stereodynamic studies in solution †

Swadhin K. Mandal,[a] G. A. Nagana Gowda,[b] Setharampattu S. Krishnamurthy *[a] and Munirathinam Nethaji[a]

[a] *Department of Inorganic and Physical Chemistry, Bangalore-560012, India*
[b] *Sophisticated Instruments Facility, Indian Institute of Science, Bangalore-560012, India*

Received 30th July 2002, Accepted 16th December 2002
First published as an Advance Article on the web 4th February 2003

The chemistry of η^3-allyl palladium complexes of pyrazolyl substituted diphosphazane ligands, $Ph_2P(E)N(R)$-$PPh(N_2C_3HMe_2$-3,5) [E = lone pair, R = $CHMe_2$ (**1**); E = lone pair, R = (*S*)-*CHMePh (**2**); E = S, R = $CHMe_2$ (**3**)] bearing a stereogenic phosphorus centre has been investigated and the complexes, $[Pd(\eta^3$-1,3-R'_2-$C_3H_3)\{\kappa^2$-$Ph_2P(E)$-$N(R)PPh(N_2C_3HMe_2$-3,5)$\}](PF_6)$ [E = lone pair or sulfur; R = $CHMe_2$ or (*S*)-*CHMePh; R′ = H, Me or Ph; **4**–**13**], have been isolated. Detailed NMR studies reveal that these complexes exist as a mixture of isomers in solution. The structures of four complexes have been determined by X-ray crystallography and only one isomer is observed in the solid state in each case. The allyl complexes formed by ligands **1** and **2** display a P,N-coordination mode except the 1,3-diphenyl allyl complex, $[Pd(\eta^3$-1,3-Ph_2-$C_3H_3)\{\kappa^2$-$Ph_2PN(CHMe_2)PPh(N_2C_3HMe_2$-3,5)$\}](PF_6)$ (**8**), which shows the presence of both P,N- and P,P-coordinated isomers in solution with the former predominating. On the other hand, the complexes bearing the diphosphazane monosulfide ligand **3** display P,S-coordination. Two-dimensional phase sensitive ^1H–^1H NOESY and ROESY measurements indicate that several of the above allyl palladium complexes undergo *syn–anti* and/or *cis–trans* isomerization in solution through an η^1-intermediate formed by the opening of the η^3-allyl group selectively at the *trans* position with respect to the phosphorus centre. Preliminary investigations show that the diphosphazanes (**1** and (*SR*)-**2**) function as efficient auxiliary ligands for catalytic allylic alkylation reactions but lead to only low levels of enantiomeric excess.

Introduction

The chemistry of palladium(II) allyl complexes is a topic of considerable contemporary interest in view of the various fluxional processes observed in these systems and also from the point of view of the potential applications of these type of complexes in asymmetric synthesis.[1] There has been a growing interest in elucidating the structures and stereodynamic behaviour of η^3-allyl palladium complexes in solution. Multinuclear and multidimensional NOE based NMR spectroscopy is a valuable tool for this purpose.[2]

The use of C_2 symmetry as a chiral auxiliary ligand design element is a well-recognised strategy for restricting the number of possible diastereomeric transition states.[3] Equally powerful stereochemical restrictions may also be realised with chiral ligands lacking C_2 symmetry through the use of electronic effects such as *trans* influence.[4] Chiral bidentate ligands incorporating strong and weak donor heteroatom pairs such as P,N-,[5] P,S-[6] or S,N-[7] have the capacity to influence both the stability and reactivity of the diastereomeric intermediates in the catalytic cycle. In the palladium catalysed allylic alkylation of symmetrically substituted allyl moiety, the regio-selectivity of nucleophilic attack determines the ratio of the enantiomeric products (Scheme 1).[8] For the mixed-donor ligand systems it is generally accepted that the nucleophilic attack takes place preferentially at the allyl terminus *trans* to the more π-accepting donor centre.[9] However, uncertainty still exists concerning the inherent reasons leading to such a site selectivity.[10]

As a part of our ongoing research on the organometallic chemistry of diphosphazane ligands,[11,12] we have recently reported the synthesis and dynamic behaviour of unsymmetrically substituted allyl palladium complexes of the diphosphazane ligands, $Ph_2PN(R)PPh(N_2C_3HMe_2$-3,5) [R = $CHMe_2$ (**1**) or R = (*S*)-*CHMePh(**2**)] bearing a stereogenic phosphorus centre and the diphosphazane monosulfide ligand $Ph_2P(S)$-$N(CHMe_2)PPh(N_2C_3HMe_2$-3,5) (**3**).[13] In this paper, we report the synthesis, structural characterisation, and dynamic behaviour of a range of cationic symmetrically substituted allyl palladium complexes of these ligands. The main purpose of this investigation is to make a systematic study of allyl palladium complexes of diphosphazane class of ligands and to investigate the roles of phosphorus chirality and *trans* influence as control elements in asymmetric catalysis involving these ligands.

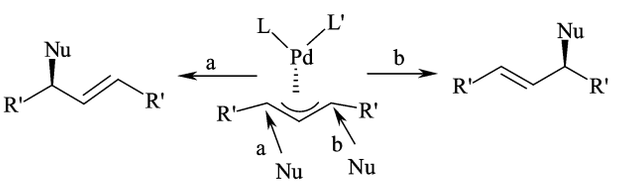

Scheme 1

Experimental

Materials and instrumentation

All reactions and manipulations were carried out under an atmosphere of dry nitrogen using standard Schlenk and vacuum-line techniques. The solvents were purified by standard procedures[14] and distilled under nitrogen prior to use. The chlorobridged palladium allyl dimers, $[Pd(\eta^3$-$C_3H_5)$-$(\mu$-$Cl)]_2$,[15] $[Pd(\eta^3$-1,3-Me_2-$C_3H_3)(\mu$-$Cl)]_2$[16] and $[Pd(\eta^3$-1,3-Ph_2-$C_3H_3)(\mu$-$Cl)]_2$[17] were prepared as previously described. The diphosphazane ligands **1**, **2** and **3** were prepared by published procedures.[11b,11e,18] In the case of **2**, the S_CR_P-diastereomer, absolute configuration of which has been determined by X-ray crystallography,[18] is used for the preparation of allyl palladium complexes unless specified otherwise. The NMR spectra were

† Organometallic chemistry of diphosphazanes. Part 17.[11g]

Electronic supplementary information (ESI) available: NMR and crystallographic data, stereodynamic behaviour schemes. See http://www.rsc.org/suppdata/dt/b2/b207447h/

DOI: 10.1039/b207447h

Table 1 Yield, melting point and elemental analysis data for η^3-allyl palladium complexes **4**–**13**

Compound	Yield (%)	Mp/°C	Elemental analyses[a]		
			C (%)	H (%)	N (%)
4	85	195–97 decomp.	46.9 (47.2)	4.6 (4.6)	5.6 (5.7)
5	90	135–38 decomp.	50.9 (51.1)	4.4 (4.5)	5.2 (5.2)
6	82	198–200 decomp.	48.7 (48.6)	5.0 (4.9)	5.6 (5.5)
7	95	204–206 decomp.	52.1 (52.2)	4.8 (4.8)	5.0 (5.1)
8	87	200–202 decomp.	55.1 (55.3)	4.6 (4.7)	4.8 (4.7)
9	74	184–87 decomp.	58.5 (58.0)	4.7 (4.6)	4.5 (4.4)
10	34	196–98 decomp.	58.7 (58.0)	4.7 (4.6)	4.6 (4.4)
11	89	178–81 decomp.	44.9 (45.3)	4.4 (4.4)	5.7 (5.5)
12	84	155–59 decomp.	46.8 (46.7)	4.8 (4.8)	5.3 (5.3)
13	77	190–93 decomp.	53.5 (53.4)	4.4 (4.6)	4.5 (4.6)

[a] Calculated values are in parentheses.

Table 2 Crystallographic data for complexes **5a**, **7a**, **8a** and **12a**

Complex	**5a**	**7a**	**8a**	**12a**
Empirical formula	$C_{34}H_{36}F_6N_3P_3Pd{\cdot}0.5CH_3COCH_3$	$C_{36}H_{40}F_6N_3P_3Pd$	$C_{41}H_{42}F_6N_3P_3Pd$	$C_{31}H_{38}F_6N_3P_3PdS$
Fw	829.01	828.02	890.09	798.01
T/K	293(2)	293(2)	293(2)	293(2)
Crystal system	monoclinic	orthorhombic	monoclinic	monoclinic
Space group	$P2_1$	$P2_12_12_1$	$P2_1/n$	$P2_1/n$
a/Å	9.2253(2)	9.474(4)	10.826(3)	9.836(5)
b/Å	37.0328(9)	19.627(4)	18.176(4)	10.758(2)
c/Å	10.9457(2)	19.837(5)	41.424(10)	33.860(9)
α/°	90.00	90.00	90.00	90.00
β/°	90.5650(10)	90.00	90.75(2)	97.03(3)
γ/°	90.00	90.00	90.00	90.00
V/Å^3	3739.3(1)	3688.5(2)	8150.0(3)	3556.0(2)
Z	4	4	8	4
Density (calcd)/Mg m^{-3}	1.473	1.491	1.451	1.491
Abs. coeff./mm^{-1}	0.685	0.694	0.634	0.773
No. refl.	15784	3638	15726	8210
Indep. refl.	10038	3638	14315	7757
Flack parameter	−0.03(2)	−0.08(5)	–	–
Final R indices: R_1, wR_2 ($I > 2\sigma_I$)	0.0383, 0.0989	0.0427, 0.1081	0.0609, 0.1604	0.0522, 0.1404
R indices (all data)	0.0441, 0.1091	0.0604, 0.1184	0.0985, 0.1846	0.0950, 0.1660

recorded using Bruker DRX-500 MHz, Bruker AMX-400 MHz and Bruker ACF-200 MHz spectrometers. Chemical shifts downfield from the reference standard were assigned positive values. Optical rotations were measured on a Jasco DIP-370 digital polarimeter. Elemental analyses were carried out using a Perkin-Elmer 2400 CHN analyser. The $^{31}P\{^1H\}$ NMR data are presented in Table 5 (see below). The ^1H and ^{13}C NMR data for the allyl moiety are listed in Tables ES1 and ES2, respectively, as Electronic Supplementary Information (ESI);† the remaining ^1H and ^{13}C NMR data are also given in the ESI.

Synthesis

[Pd(η^3-C_3H_5){κ^2-$Ph_2PN(CHMe_2)PPh(N_2C_3HMe_2$-3,5)}](PF$_6$), 4. A mixture of 0.036 g (0.98×10^{-4} mol) of [Pd(η^3-C_3H_5)(μ-Cl)]$_2$, 0.033 g (2.02×10^{-4} mol) of NH_4PF_6 and 0.095 g (2.13×10^{-4} mol) of **1** was dissolved in 20 cm^3 of acetone. The solution was stirred for 2 h at 298 K and the white precipitate formed during the reaction was filtered off. The resulting colourless filtrate was concentrated under reduced pressure to 10 cm^3 and the solution was layered by adding 10 cm^3 of hexane (bp 40–60 °C) to yield colourless crystals. The other allyl palladium complexes, **5**–**13** were synthesised by an analogous procedure by varying the allyl palladium chloro dimer and the diphosphazane ligand. The yields, melting points and elemental analyses for these complexes are given in Table 1.

X-Ray crystallography

Crystal data for complex **5a** was collected using Siemen's SMART-CCD diffractometer. The intensity data for complexes **7a**, **8a** and **12a** were collected using an Enraf-Nonius CAD-4 diffractometer. The crystallographic data and details of data collections are summarised in Table 2. The structures were solved by Patterson's heavy atom method using the program SHELXS 86[19] and refined on F^2 values for all unique data by full-matrix least-squares using SHELXS 97.[20] The non-hydrogen atoms were refined anisotropically. The hydrogen atoms were fixed at their calculated geometrical positions and allowed to ride on the non-hydrogen atoms to which they are attached. The validity of the absolute structure for **5a** and **7a** was established by the method of Flack.[21]

CCDC reference numbers 190877–190880.

See http://www.rsc.org/suppdata/dt/b2/b207447h/ for crystallographic data in CIF or other electronic format.

General procedure for palladium-catalysed allylic alkylation

The ligand (2.5 mol%) and [Pd(η^3-C_3H_5)(μ-Cl)]$_2$ (1 mol%) were dissolved in 4 cm^3 of degassed (by three freeze–thaw cycles) CH_2Cl_2. A solution of (*rac*)-1,3-diphenyl-2-propenyl acetate (I) or (*E*)-1-phenyl-2-propenyl acetate (III) (1 equiv.), in 2 cm^3 CH_2Cl_2, was added followed by dimethyl malonate (2 equiv.), N,O-bis(trimethylsilyl)acetamide (2 equiv.), and a catalytic amount of KOAc. The mixture was stirred at 298 K for 24 h and the reaction was monitored by TLC. A saturated aqueous solution of NH_4Cl (10 cm^3) was added to the reaction mixture and the organic part was extracted with diethyl ether (10×3 cm^3). The ether extract was filtered over activated celite, washed with water (3×10 cm^3) and dried over anhydrous Na_2SO_4. Solvent was removed from the ether extract under reduced pressure and the crude product was purified by column chromatography over silica gel (eluent hexane/ethyl acetate,

9 : 1). The optical rotation was measured for the product, PhCH=CH–CHPh{$CH(CO_2Me)_2$} (II) and the enantiomeric excess (e.e.) was calculated from the optical rotation value using the literature data.[6b,22] The enantiomeric excesses obtained were 29 ± 2% in favour of the '*R*' enantiomer (observed $[\alpha]_D$ = + 6.10, *c* = 3.2, EtOH) when ligand **1** was used and 28 ± 2% in favour of the '*S*' enantiomer (observed $[\alpha]_D$ = −5.96, *c* = 3.2, EtOH) when ligand (*SR*)-**2** was used as the chiral auxiliary.

Results and discussion

The cationic allyl palladium complexes **4**–**13** have been prepared from the reactions of the chlorobridged palladium allyl dimers, $[Pd(\eta^3\text{-}1,3\text{-}R'_2\text{-}C_3H_3)(\mu\text{-}Cl)]_2$ (R′ = H or Me or Ph) with the appropriate ligands in the presence of NH_4PF_6 in acetone (Scheme 2). These complexes have been characterised by elemental analyses and NMR spectral data (see ESI† and Table 5 below). The isomeric composition in each case has been determined from NMR spectroscopy. The salient features of the spectroscopic data and dynamic behaviour are discussed below.

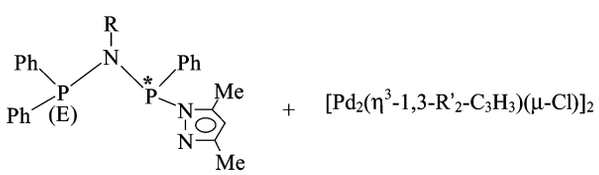

1, R = $CHMe_2$, E = lone pair (l.p);
2, R = (*S*)-*CHMePh, E = l.p;
3, R = $CHMe_2$, E = S

NH_4PF_6

$[Pd(\eta^3\text{-}1,3\text{-}R'_2\text{-}C_3H_3)$(**1** or **2** or **3**)$](PF_6)$

4, R' = H, R = $CHMe_2$, E = l.p;
5, R' = H, R = (*S*)-*CHMePh, E = l.p;
6, R' = Me, R = $CHMe_2$, E = l.p;
7, R' = Me, R = (*S*)-*CHMePh, E = l.p;
8, R' = Ph, R = $CHMe_2$, E = l.p;
9, R' = Ph, R = (*S*)-*CHMePh, E = l.p;
10, R' = Ph, R = (*S*)-*CHMePh, E = l.p; (S_cS_p-diastereomer)
11, R' = H, R = $CHMe_2$, E = S;
12, R' = Me, R = $CHMe_2$, E = S;
13, R' = Ph, R = $CHMe_2$, E = S

Scheme 2

Palladium allyl complexes of $Ph_2PN(R)PPh(N_2C_3HMe_2\text{-}3,5)$ [R = $CHMe_2$ (1) or (*S*)-*CHMePh (2)]

The $^{31}P\{^1H\}$ NMR spectra of **4** and **5** in $CDCl_3$ show two AX spin patterns indicating the presence of two isomers in solution. The relative ratios of the isomers are 3 : 1 and 3.4 : 1 for **4** and **5**, respectively. An analysis of ^{13}C NMR spectra of allyl carbons clearly shows P,N-coordination *via* the nitrogen atom of the pyrazole ring instead of the usually observed P,P-coordination.[11c–e] A doublet is observed for each of the two terminal allyl carbon nuclei. The resonances of the terminal allyl carbon nuclei *trans* to the coordinated phosphorus centre appear in the range *ca.* 75–81 ppm with a ^2J(P,C) of 28–31 Hz which lies in a region usually observed for *trans* ^{31}P–^{13}C coupling whereas the signal for the terminal allyl carbon nucleus *trans* to nitrogen resonates in a more shielded region (*ca.* 58–62 ppm) with a ^2J(P,C) coupling constant of the order of 3–4 Hz which is typical for a two-bond *cis* coupling of phosphorus and carbon nuclei.[23] The resonances of the central allyl carbon nuclei of all the isomers appear as doublets as would be expected for P,N-coordination. The driving force for the P,N-coordination might be the formation of a stable six-membered ring around palladium rather than a four-membered ring which would result from P,P-coordination. Moreover, electronically the coordination of the σ-donor nitrogen is more favourable than that of the π-acceptor phosphorus as it can synergistically enhance the metal–allyl bonding.[24]

Detailed 2D NMR studies (^1H–^1H DQF-COSY, NOESY, ROESY and ^{13}C–^1H HSQC) show that the two isomers of **4** and **5** have the *endo*- (major) and *exo*- (minor) configurations (Fig. 1).[2b,25] For the major isomers of **4** and **5**, there is a NOE contact between the 3-Me protons of pyrazole and the central allyl proton, H_c and the *syn* proton H_s. This result indicates that the central allyl hydrogen, H_c points toward 3-Me protons of pyrazole *i.e.* the major isomers (**4a** and **5a**) have the *endo*-configuration (3-Me protons and H_c are on the same side of the N–Pd–P coordination plane). By contrast, the pyrazole 3-Me protons of the minor isomers of **4** and **5** do not show NOE contact to the central allyl proton H_c but there is a strong NOE contact to the *anti* allyl proton, H_a. Hence, the minor isomers (**4b** and **5b**) are assigned the *exo*-configuration (3-Me and H_c are on the opposite sides of the N–Pd–P coordination plane).

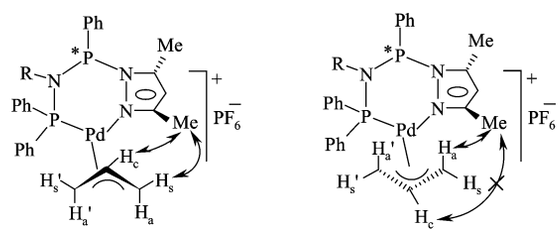

endo-; (**4a**, **5a**) *exo*-; (**4b**, **5b**)

Fig. 1 The two isomers of Pd(II)–allyl diphosphazane complexes, $[Pd(\eta^3\text{-}C_3H_5)\{\kappa^2\text{-}Ph_2PN(R)PPh(N_2C_3HMe_2\text{-}3,5)\}](PF_6)$ [R = $CHMe_2$-(**4**), (*S*)-*CHMePh(**5**)] observed in solution. Selective NOE contacts reveal that in the *endo*-isomer, the central allyl proton and pyrazole-3-Me protons are close to each other whereas for the *exo*-isomer, such an NOE contact with the central allyl proton is absent.

The phase sensitive ^1H–^1H 2D NOESY and ROESY spectra of **4** at 298 K clearly reveal *syn–anti* exchange of the allyl protons *trans* to nitrogen. Pregosin and coworkers[26] have demonstrated that such an exchange can be explained by a selective opening of the η^3-allyl moiety *trans* to the coordinated phosphorus centre followed by rotation around the sp^3–sp^2 C–C bond and reversal to the η^3-mode of coordination by the other face of the allyl moiety. Complex **5** does not show any dynamic behaviour at 298 K; presumably the interconversion is slow on the NMR time scale at this temperature. However, at 323 K, the ^1H–^1H 2D NOESY and ROESY spectra of **5** indicate the presence of two simultaneous exchange processes. Close examination of the allyl proton exchange cross-peaks reveals selective *syn–anti* exchange as well as *cis–trans* isomerisation. The observed exchange results can be accounted for by considering the sequence of steps shown in Scheme 3. Step (i) is the selective opening of the η^3-allyl bond to the metal at the carbon *trans* to the coordinated phosphorus centre of **5a** to generate the intermediate **D**. This intermediate (**D**) can undergo either a rotation around the sp^3–sp^2 C–C bond to form **5b** [step (ii)] or it can undergo a rotation around the Pd–C bond [step (iii)] thus resulting in **5c**. The isomers **5b** and **5c** are essentially the same and are not distinguishable in the NMR spectrum, as the allyl group is unsubstituted and symmetrical. Thus the isomerisation appears to be subject to electronic control as observed for η^3-allyl palladium complexes of other heterodonor P,S-,[27] P,O-[28] and P,N-[23b,29] bidentate ligand systems.

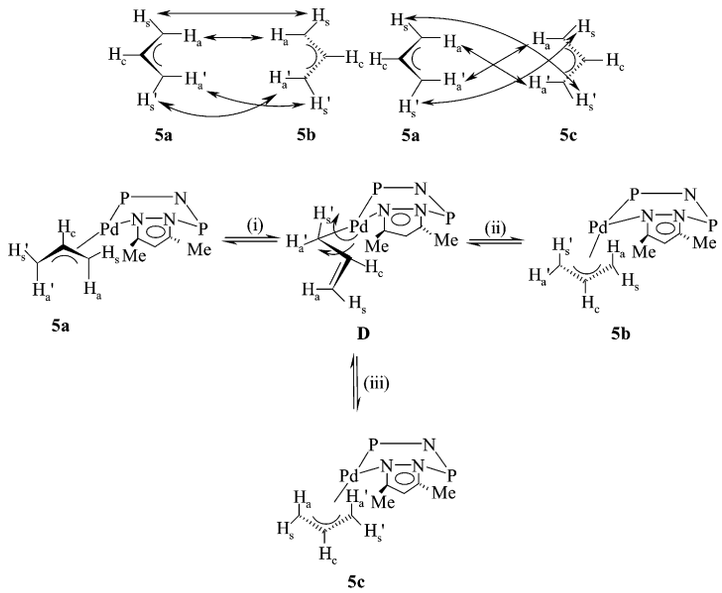

Scheme 3

When a solution of complex **5** in acetone/hexane (1 : 1 v/v) is cooled, crystals of **5a** are obtained. The crystallographic data for **5a** are summarised in Table 2. Selected bond lengths and bond angles are listed in Table 3. The solid state structure shows the presence of two crystallographically independent molecules **5a**(**A**) and **5a**(**C**) (**A** and **C** represent the diastereomeric configuration as explained below) shown in Fig. 2. The 'PdC$_2$PN' core shows a distorted square-planar geometry with bond distances of Pd–C, Pd–P and Pd–N in the expected range for Pd(II) allyl compounds with P,N-chelate ligands. The P–N–P bond angle is expanded to 121.8(2)° which is normally *ca.* 100° for P,P-coordinated complexes.[11] The relative orientations of the chelating ligand and the allyl moiety are similar in both the molecules. The central allyl carbon and 3-methyl group of the pyrazole ring in **5a**(**A**) lie above the coordination plane defined by N–Pd–P whereas in **5a**(**C**) they are located below this plane. The two molecules are not superimposable; the molecular asymmetry arises because of the presence of chiral centres in the diphosphazane ligand and the position of the η^3-coordinated allyl moiety which is obliquely placed with respect to the metal square plane.[30,31] The configuration at the stereogenic palladium centre in **5a**(**A**) and **5a**(**C**) can be designated as **A** and **C**, respectively, following the method adopted by Lanza *et al.*[30] When the molecule is viewed from the central allyl carbon towards palladium, the other two atoms coordinated to the metal *viz.* P and N (with decreasing CIP priority) follow an anticlockwise direction in **5a**(**A**) whereas these atoms follow a clockwise direction in **5a**(**C**) (see Fig. 2). The six-membered ring in both the molecules adopts a distorted boat conformation. The difference between the two Pd–C bond distances indicates the greater *trans* influence of the phosphorus donor compared to nitrogen. The Pd–C bond lengths *trans* to the coordinated phosphorus centre are 2.213(7) and 2.189(7) Å whereas for the Pd–C bond *trans* to nitrogen are 2.127(8) and 2.107(7) Å for **5a**(**A**) and **5a**(**C**), respectively (see Table 3).[10,23b,32] This elongation of Pd–terminal allyl carbon bond length *trans* to the coordinated phosphorus centre as compared to that *trans* to nitrogen is consistent with the proposed mechanism involving selective opening of one of the allyl termini.

To obtain a better understanding of the fluxional process, we have studied 1,3-disubstituted allyl complexes of the ligands **1** and **2** since the unsubstituted allyl moiety is a poor model to understand the stereodynamic process. The various possible allylic arrangements are shown in Scheme 4. For each arrangement, there is also the possibility of *exo*- or *endo*-isomers (Scheme 5). Furthermore, there is the possibility of P,P-coordination.

Table 3 Selected bond distances (Å) and angles (°) in **5a**, **7a**, **8a** and **12a**

Bond distances/Å		Bond angles/°	
Molecule **5a**(**A**)			
Pd(1)–C(1)	2.127(8)	P(4)–Pd(1)–N(4)	86.2(1)
Pd(1)–C(2)	2.133(7)	C(1)–Pd(1)–C(3)	67.9(4)
Pd(1)–C(3)	2.213(7)	C(3)–Pd(1)–P(4)	172.0(3)
Pd(1)–P(4)	2.297(1)	C(1)–Pd(1)–N(4)	169.5(3)
Pd(1)–N(4)	2.100(5)	P(2)–N(6)–P(4)	121.8(2)
Molecule **5a**(**C**)			
Pd(2)–C(38)	2.107(7)	P(3)–Pd(2)–N(1)	86.6(1)
Pd(2)–C(39)	2.155(8)	C(38)–Pd(2)–C(40)	67.9(4)
Pd(2)–C(40)	2.189(7)	C(40)–Pd(2)–P(3)	171.0(3)
Pd(2)–P(3)	2.296(1)	C(38)–Pd(2)–N(1)	169.7(3)
Pd(2)–N(1)	2.116(5)	P(5)–N(5)–P(3)	121.8(2)
Complex **7a**			
Pd(1)–C(4)	2.12(1)	P(2)–Pd(1)–N(3)	84.2(2)
Pd(1)–C(3)	2.129(8)	C(4)–Pd(1)–C(2)	66.3(5)
Pd(1)–C(2)	2.27(1)	C(2)–Pd(1)–P(2)	172.2(4)
Pd(1)–P(2)	2.304(2)	C(4)–Pd(1)–N(3)	168.8(4)
Pd(1)–N(3)	2.150(6)	P(1)–N(1)–P(2)	121.6(3)
Molecule **8a**(**A**)			
Pd(1)–C(3)	2.173(7)	P(1)–Pd(1)–N(3)	84.2(2)
Pd(1)–C(2)	2.179(7)	C(3)–Pd(1)–C(1)	66.5(3)
Pd(1)–C(1)	2.224(7)	C(1)–Pd(1)–P(1)	176.4(2)
Pd(1)–P(1)	2.328(2)	C(3)–Pd(1)–N(3)	165.6(3)
Pd(1)–N(3)	2.119(6)	P(1)–N(1)–P(2)	122.8(3)
Molecule **8a**(**C**)			
Pd(2)–C(44)	2.148(7)	P(3)–Pd(2)–N(6)	83.9(2)
Pd(2)–C(43)	2.178(8)	C(44)–Pd(2)–C(42)	67.1(3)
Pd(2)–C(42)	2.232(8)	C(42)–Pd(2)–P(3)	174.2(2)
Pd(2)–P(3)	2.306(2)	C(44)–Pd(2)–N(6)	168.2(3)
Pd(2)–N(6)	2.128(6)	P(3)–N(4)–P(4)	121.9(4)
Complex **12a**		Complex **12a**	
Pd(1)–C(2)	2.171(7)	P(1)–Pd(1)–S(1)	91.7(4)
Pd(1)–C(3)	2.127(5)	C(2)–Pd(1)–C(4)	67.4(3)
Pd(1)–C(4)	2.192(6)	C(4)–Pd(1)–P(1)	167.7(2)
Pd(1)–P(1)	2.262(1)	C(2)–Pd(1)–S(1)	163.6(2)
Pd(1)–S(1)	2.338(1)	P(1)–N(1)–P(2)	118.3(2)

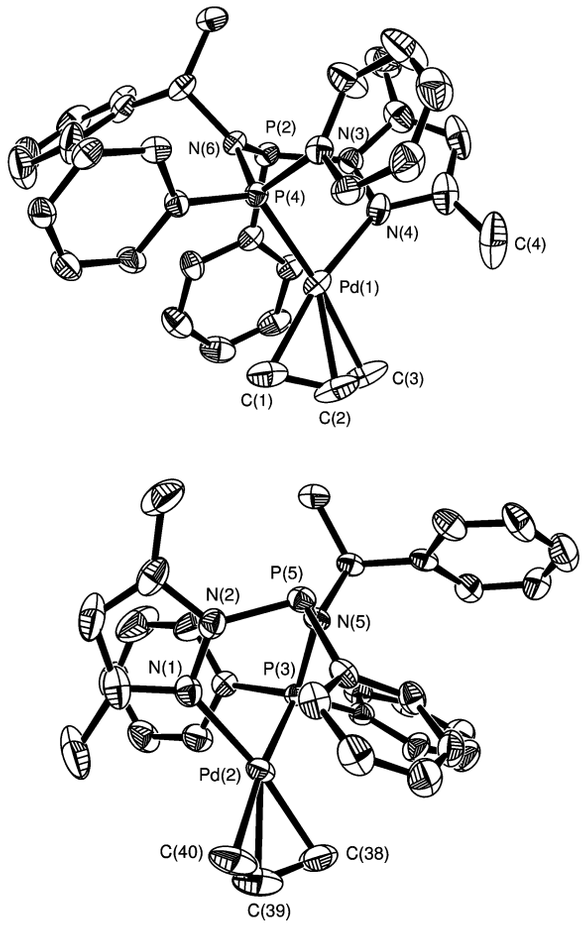

Fig. 2 A view of the molecular structure of **5a**, showing the presence of two independent molecules **5a**(**A**) (top) and **5a**(**C**) (bottom) (the hexafluorophosphate anion, the hydrogen atoms and the lattice held Me_2CO are not shown).

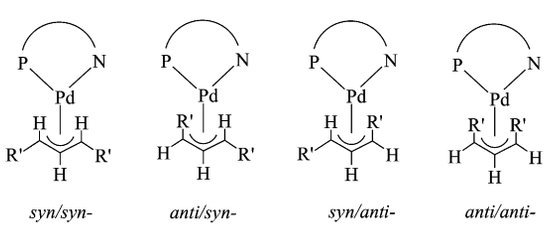

Scheme 4

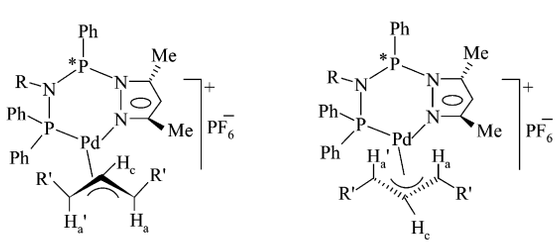

Scheme 5

The complexes, $[Pd(\eta^3\text{-}1,3\text{-}Me_2\text{-}C_3H_3)(\mathbf{1})](PF_6)$ (**6**) and $[Pd(\eta^3\text{-}1,3\text{-}Me_2\text{-}C_3H_3)((SR)\text{-}\mathbf{2})](PF_6)$ (**7**) exist as a mixture of four isomers as shown by their $^{31}P\{^1H\}$ NMR spectra. A detailed analysis of the ^{13}C, ^1H and $^{31}P\{^1H\}$ NMR spectra confirms that all the four isomers are P,N-coordinated species. The isomeric distributions are 43 : 35 : 15 : 7 and 69 : 19 : 9 : 3 for **6** and **7**, respectively. Two-dimensional NMR studies have been carried out for complex **7**. The assignment of the allyl configuration is based on ^1H spin–spin coupling constants and intra-allyl NOESY cross-peaks. (Two strong NOE cross-peaks between the central allylic proton with two terminal allyl methyl protons indicate a *syn*/*syn*-arrangement while a strong NOE between the central allylic proton and one of the two terminal allyl protons indicates *syn*/*anti*- or *anti*/*syn*-arrangements.) Appearance of an NOE cross-peak between the central allyl proton and 3-methyl protons of pyrazole moiety would reveal the *endo*-configuration, whereas the absence of such an NOE involving the central allyl proton would clearly point to the *exo*-configuration. Additionally, the chemical shift of the central allyl proton for the *endo*-isomer appears in a deshielded region (*ca.* 5.5 ppm) compared to that for the *exo*-isomer (*ca.* 4 ppm) as observed for complexes **4** and **5**. Based on the above considerations, we assign the major species as *endo*, *syn*/*syn*- (**6a** and **7a**), the second minor species as *exo*-, *syn*/*syn*- (**6b** and **7b**), the third minor species as *exo*, *anti*/*syn*- (**6c** and **7c**) and the fourth minor species as *endo*, *anti*/*syn*- (**6d** and **7d**) isomers (see Fig. 3). The absence of the *anti*/*anti*-isomer is understandable on the basis of steric grounds but the absence of any *syn*/*anti*-isomer is most probably due to electronic reasons. The *anti* allyl methyl group is invariably present at the *trans* position with respect to the nitrogen donor. This is in accord with the proposed mechanism for the exchange processes observed for **4** and **5** (Scheme 3), in which the sp^3 carbon is generated at the *trans* position with respect to the nitrogen donor; in other words, the η^3-allyl group opens selectively at the *trans* position with respect to the coordinated phosphorus donor to form the 'η^1-coordinated' intermediate.

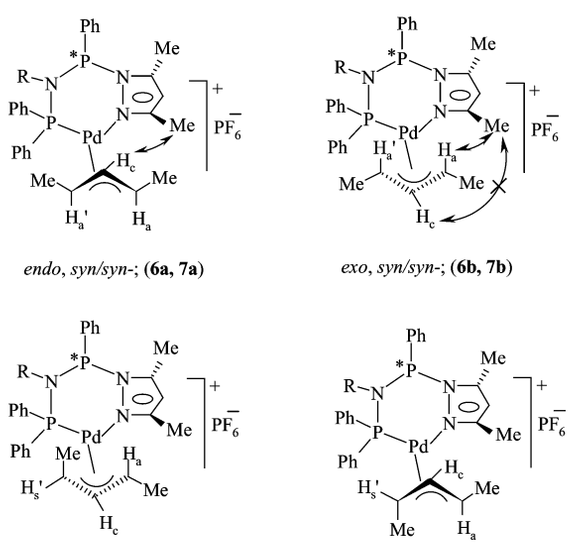

Fig. 3 The four isomers observed in solution for 1,3-dimethyl allyl palladium complexes, $[Pd(\eta^3\text{-}1,3\text{-}Me_2\text{-}C_3H_3)\{\kappa^2\text{-}Ph_2PN(R)PPh(N_2C_3HMe_2\text{-}3,5)\}](PF_6)$ [R = $CHMe_2$ (**6**), (*S*)-*CHMePh (**7**)].

Although complex **7** exists as a mixture of four diastereomers in solution, the solid state structure shows that the allyl moiety adopts an *endo*, *syn*/*syn*-configuration (**7a**) (*endo*- refers to the relative orientation of the central C–H vector pointing towards the 3-methyl group on the pyrazole ring). The crystallographic data are listed in Table 2. The molecular structure is shown in Fig. 4. The bonding parameters (Table 3) fall in the expected ranges.[23b,31] A few structural features are worth noting. If one considers the inner coordination sphere as formed by the P and N donor atoms of the diphosphazane ligand and by the terminal allyl carbons C(2) and C(4), the coordination geometry around the metal centre is distorted square planar, with the P(2)–Pd(1)–N(3) and C(4)–Pd(1)–C(2) angles being 84.2(2) and 66.3(5)°, respectively. The two terminal allyl carbon atoms are not coplanar with the coordination plane formed by N(3)–Pd(1)–P(2); the distances of C(2) and C(4) from this plane are

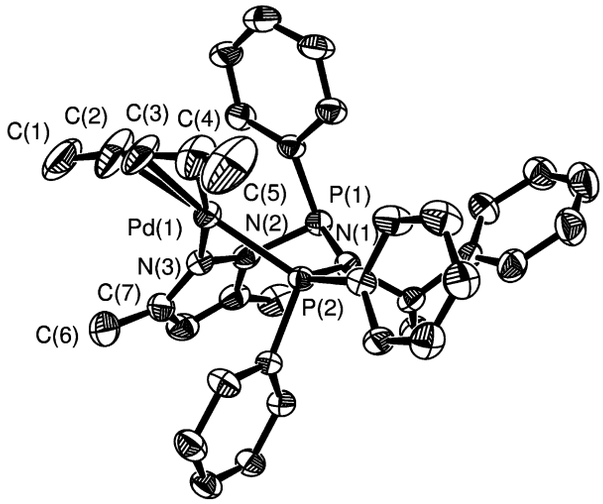

Fig. 4 A view of the molecular structure of complex **7a** (the hydrogen atoms and the hexafluorophosphate anion are not shown).

0.16 and 0.07 Å, respectively. The central allyl carbon atom C(3) is located at a distance of 0.36 Å from the same plane. The 3-Me pyrazole carbon, C(6) lies on the same side of the central allyl carbon with regard to the coordination plane (distance from the coordination plane is 2.23 Å). The terminal Pd–C allyl bond lengths are significantly different from one another; the carbon atom *trans* to the coordinated phosphorus centre displays the expected longer distance [Pd(1)–C(2) = 2.27(1) Å], as compared to its partner *trans* to nitrogen [Pd(1)–C(4) = 2.12(1) Å] (Table 3). This is a reflection of the higher *trans* influence [10,32,33] of the phosphorus donor centre. The six-membered chelate ring adopts a distorted boat conformation as shown by the distance calculation from the mean plane defined by N(1)–N(2)–N(3); both Pd(1) and P(1) lie above the N(1)–N(2)–N(3) plane (the deviations from this plane are 1.17 and 0.74 Å respectively) whereas P(2) atom is almost coplanar with this plane (the deviation is only 0.10 Å below this plane).

When crystalline **7a** is dissolved in $CDCl_3$ at 298 K, it undergoes slow isomerisation (not detectable by phase sensitive ^{1}H–^{1}H NOESY and ROESY spectra at 298 K) to produce **7b**, **7c** and **7d**. The formation of *exo*, *syn*/*syn*-isomer (**7b**) from the *endo*, *syn*/*syn*-isomer (**7a**) can be rationalised by considering a rotation around the Pd–C bond (step (i), Scheme 6). Thus complex **7b** represents **5c** shown in the isomerisation pathway for unsubstituted allyl complexes (see Scheme 3). The *exo*, *anti*/*syn*-isomer (**7c**) is the 1,3-dimethyl substituted analogue of **5b** which is formed by rotation around sp^3–sp^2 C–C bond (step (ii), Scheme 6). Formation of **7d** can be explained by considering a further *syn–anti* exchange process starting from **7b** (step (iii), Scheme 6). This isomerisation pathway is supported by the ^{1}H–^{1}H NOESY and ROESY spectra at 323 K for complex **7**. The exchange results at 323 K reveal that complex **7a** undergoes exchange with complex **7b** by *cis–trans* isomerisation and at the same time complex **7b** also shows fluxional behaviour with complex **7d** by *syn–anti* isomerisation pathway (on the basis of exchange pattern observed for the allyl methyl groups of the two isomers). There is no observable exchange between **7a** and **7c** at 323 K.

When we move to the 1,3-diphenyl allyl system containing the more bulky substituents with enhanced electron donating capacity compared to the 1,3-dimethyl allyl system, the complex formed by the diphosphazane ligand **1**, *viz.* [Pd(η^3-1,3-Ph_2-C_3H_3){κ^2-$Ph_2PN(CHMe_2)PPh(N_2C_3HMe_2$-3,5)}]($PF_6$) (**8**) exists as a mixture of three isomers in solution in the ratio 75 : 15 : 10 as shown by its ^{31}P{^{1}H} and ^{1}H NMR spectra. The ^{13}C NMR and ^{1}H–^{1}H NOESY spectra show that the major component is the P,N-coordinated *endo*, *syn*/*syn*-isomer (**8a**) and the other two minor isomers (**8b** and **8c**) are P,P-coordinated diastereomers (shown in Fig. 5). The magnitude of ^2J(P,P) for P,N-coordination (*ca.* 30 Hz) is much less than that for P,P-coordination (*ca.* 115 Hz). Such a large difference in ^2J(P,P) is probably due to the difference in P–N–P bond angle in the two cases. The assignment of the resonances arising from the two minor isomers (**8b** and **8c**) are based on the chemical shift difference of two methyl groups at 3- and 5-positions of the pyrazole ring. The value of the chemical shift difference $\Delta\delta(CH_3)$ [δ(5-CH_3) − δ(3-CH_3)] for the isomer **8b** is 1.10 ppm whereas this difference for the isomer **8c** is 0.16 ppm. Such a large difference indicates that in **8b** the central allyl carbon and pyrazole ring are on the same side of the P–Pd–P coordination plane and the allyl phenyl group comes close to one of the pyrazole methyl groups. Thus the two methyl groups experience different steric and electronic environments. By contrast, the phenyl groups and the pyrazole methyl groups in **8c** are on opposite sides of the coordination plane resulting in lesser extent of interaction of the pyrazole methyl groups with the allylic moiety. The 1,3-diphenyl allyl complexes of the more bulky diphosphazane ligands, (*SR*)-Ph_2PN((*S*)-*CHMePh)PPh($N_2C_3HMe_2$-3,5) and (*SS*)-Ph_2PN((*S*)-*CHMePh)PPh($N_2C_3HMe_2$-3,5) form only the P,N-coordinated isomers **9** and **10** with *endo*, *syn*/*syn*-configuration as revealed by ^{1}H–^{1}H NOESY NMR spectra. The formation of only one isomer is not surprising as the *syn*/*anti*- or *anti*/*anti*-arrangements are not favourable for allylic moiety containing bulky phenyl groups.

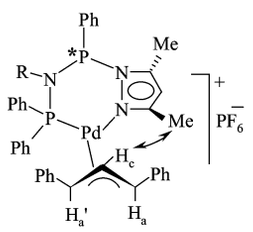

endo, *syn/syn*-; (**8a, 9, 10**)

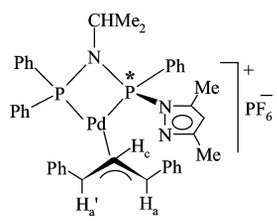

endo, *syn/syn*-; (**8b**)

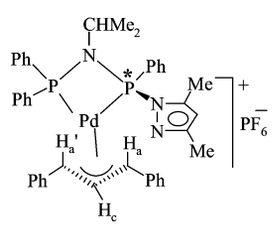

exo, *syn/syn*-; (**8c**)

Fig. 5 The isomeric species observed in solution for the 1,3-diphenyl allyl palladium(II) diphosphazane complexes, [Pd(η^3-1,3-Ph_2-C_3H_3){κ^2-$Ph_2PN(R)PPh(N_2C_3HMe_2$-3,5)}](PF_6) [R = $CHMe_2$ (**8**), (*S*)-*CHMePh (**9**, **10**)].

The molecular structure of complex **8** reveals that only the *endo*, *syn*/*syn*-isomer (**8a**) is present in the solid state. The crystal data are given in Table 2 and selected bond angles and bond distances are listed in Table 3. There are two independent molecules in the unit cell, which are not superimposable. An ORTEP plot of the two molecules is shown in Fig. 6. Both the molecules feature P,N-coordination. Furthermore, the central allyl carbon points towards the 3-methyl of the pyrazole ring revealing an *endo*-configuration with *syn*/*syn*-arrangement of the allyl phenyl groups in both the molecules **8a**(**A**) and **8a**(**C**). The two molecules differ in their relative direction of P–Pd–N when the molecule is viewed from the central allyl carbon towards palladium; in **8a**(**A**) it follows an anticlockwise direction whereas in **8a**(**C**) it is in the clockwise direction. The coordination geometry around the palladium metal is distorted square planar, with the allyl ligand markedly displaced from its idealised position. In molecule **8a**(**A**), the two terminal carbon

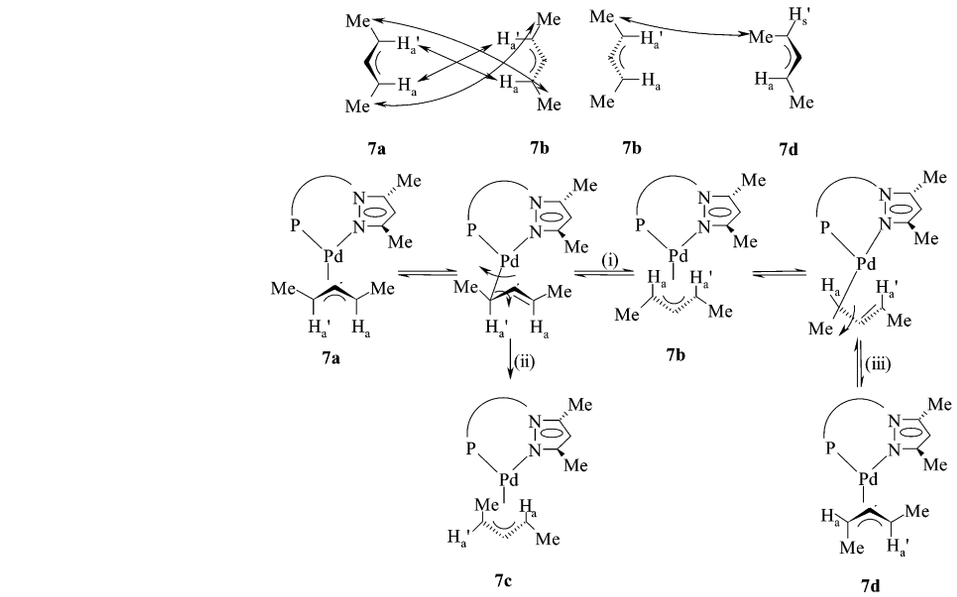

Scheme 6

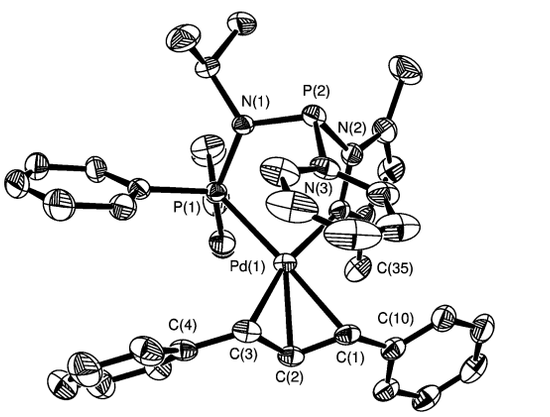

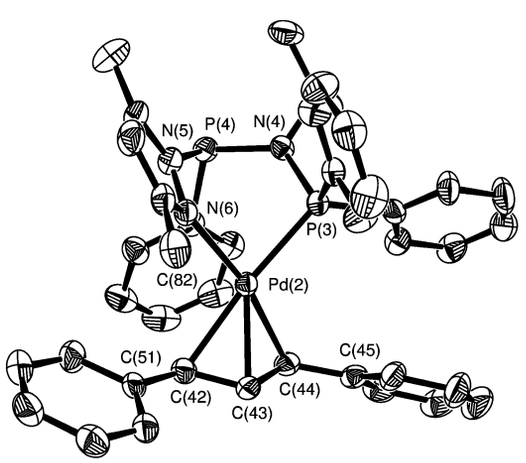

Fig. 6 A view of the molecular structure of **8a** showing the presence of two independent molecules **8a**(**A**) (top) and **8a**(**C**) (bottom) (the hydrogen atoms and the hexafluorophosphate anion are not shown).

atoms are on the same side of the coordination plane formed by N(3)–Pd(1)–P(1) (the distances are 0.01 and 0.12 Å for C(1) and C(3) respectively) and the central allyl carbon atom C(2) resides on the opposite side (the distance is 0.61 Å). On the other hand, in molecule **8a**(**C**), the terminal allyl carbons are located on opposite sides to the plane formed by N(6)–Pd(2)–P(3) (the distances are 0.06 and 0.115 Å for C(42) and C(44) respectively). The central allyl carbon, C(43) is located at a distance of 0.65 Å from the coordination plane on the same side of C(42), as shown below:

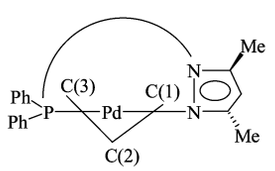

molecule **8a**(**A**)

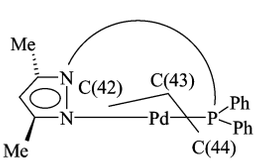

molecule **8a**(**C**)

The deviation of the terminal carbon atoms from the coordination plane is less for the carbon atom *trans* to the coordinated phosphorus than the one *trans* to nitrogen. The plane of the allyl ligand is tilted (20.4° in molecule **8a**(**A**) and 20.3° in molecule **8a**(**C**)) from an axis perpendicular to the N–Pd–P coordination plane. The allyl ligands are rotated markedly around the Pd–allyl bond axis away from the $-PPh_2$ group to minimise steric interaction with the allyl phenyl groups. A similar rotation of the allyl moiety with respect to its idealised position has also been observed in the related cationic complexes with P,N-chelating ligands, containing the sterically demanding η^3-1,3-diphenylallyl fragment.[10,23a,32] As expected, the palladium–terminal allyl carbon bond distance, which is *trans* to the coordinated phosphorus, is longer than that *trans* to nitrogen in both the molecules, revealing the greater *trans* influence of the phosphorus donor centre. The chelated six-membered rings adopt boat conformations.

When a crystalline sample of complex **8a** is dissolved in $CDCl_3$, it undergoes slow isomerisation to produce a mixture of complexes **8a**–**c**. The phase sensitive ^1H–^1H NOESY spectrum at 298 K indicates no observable exchange between these isomers which is not surprising as the sterically demanding allyl moiety raises the activation barrier for exchange. When the temperature is raised (323 K), one observes an exchange between the isomers **8b** and **8c** probably *via* a *cis*–*trans* isomerisation. The formation of **8b** and **8c** from **8a** (the isomer present in the solid state) can be rationalised by considering a pathway as shown in Scheme 7. Alternatively, **8b** may be formed first and then it can undergo *cis*–*trans* isomerisation to form **8c**. When the ^1H NMR spectrum is recorded immediately after dissolving the solid **8a** in $CDCl_3$, the three isomers **8a**–**8c** are present in the ratio 91 : 4 : 3. This ratio changes to 75 : 14 : 11 upon heating the sample at 323 K for 1 h. It may be noted that the relative ratio of **8b** and **8c** remains the same before and after the

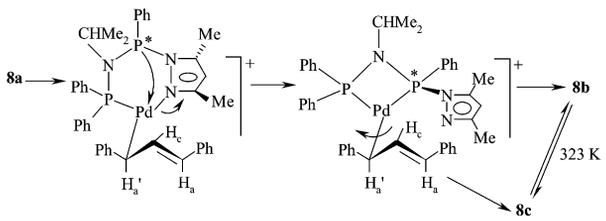

Scheme 7

equilibrium is attained although the relative ratios with respect to **8a** vary. This result indicates that the formation of **8b** and **8c** from **8a** involves a common intermediate formed by selective opening of the allyl terminus *trans* to the coordinated phosphorus centre accompanied by a concerted attack of the metal by the non-coordinated phosphorus. Recombination to the η^3-mode before and after a rotation around the Pd–C bond would generate **8b** and **8c**, respectively (Scheme 7).

Palladium allyl complexes of a diphosphazane monosulfide ligand, $Ph_2P(S)N(CHMe_2)PPh(N_2C_3HMe_2$-3,5) (3)

The unsymmetrically substituted diphosphazane monosulfide ligand, $Ph_2P(S)N(CHMe_2)PPh(N_2C_3HMe_2$-3,5) (**3**) consists of three potential donor centres namely, S, P and N at the 2-position of the pyrazole ring. It can form complexes using either P,N- or P,S- or N,S-combinations for binding to the metal resulting in a four-, five- or seven-membered chelate ring, respectively, around the metal. The $^{31}P\{^1H\}$ NMR spectrum of the complex, $[Pd(\eta^3\text{-}C_3H_5)\{\kappa^2\text{-}Ph_2P(S)N(CHMe_2)PPh(N_2C_3HMe_2$-3,5)$\}](PF_6)$ (**11**) in $CDCl_3$ shows two pairs of doublets in a ratio 4 : 1 revealing the presence of two diastereomers. The ^{13}C allyl resonances are assigned unequivocally by carrying out a ^{13}C–^1H HSQC 2D experiment with the help of pre-assigned allyl ^1H resonances by a ^1H–^1H COSY experiment. Analysis of the ^{13}C NMR spectrum shows a doublet pattern with a $^2J(P,C)$ value of *ca.* 30 Hz for one of the two terminal allyl carbon resonances in case of isomers **11a** and **11b** indicating bonding of one phosphorus with the palladium centre. From the ^{31}P chemical shifts (Table 5), we can conclude that the pyrazol-bearing phosphorus atom and the sulfur atom are coordinated to palladium. The doublet at *ca.* 91.5 ppm is assigned the coordinated $-PPh(N_2C_3HMe_2$-3,5) phosphorus nucleus with coordination shift of 26.0 ppm as compared with the free ligand ^{31}P chemical shift. The second doublet at *ca.* 77.0 ppm with a coordination shift of 6.5 ppm is assigned the non-coordinated $-P(S)Ph_2$ phosphorus nucleus. This conclusion is supported by the ^{13}C chemical shifts of the allyl carbon nuclei when compared with the chemical shifts of allyl carbon nuclei of P,N-coordinated complexes **4**–**10** (see ESI). It may be noted that the chemical shifts of allyl carbon nuclei *trans* to nitrogen are more shielded (by ~10–20 ppm) than the chemical shifts of the allyl carbon nuclei *trans* to sulfur when we consider the similar allyl isomers in both the cases. Thus, in contrast to **1** and **2**, the ligand **3** does not coordinate through the nitrogen atom of the pyrazole ring. The P,S-coordination is presumably favoured because of the formation of a stable five-membered ring around the palladium centre. The competitive N,S-coordination would lead to the formation of a seven-membered chelate ring around the palladium atom.

Two sets of five non-equivalent η^3-allyl proton resonances are observed in the ^1H NMR spectrum of **11** at 298 K. Some of the ^1H resonances of the minor isomer **11b** (*e.g.* H_c and H_a) overlap with those arising from the major isomer (**11a**), but they can be located by 2D NMR ^1H–^1H NOESY measurements. The most interesting NOE interaction is that observed between the 5-CH_3 group of the pyrazole ring and the central allyl proton, H_c and *syn* allyl proton *trans* to the sulfur atom, H_s' for the major isomer (**11a**) revealing an *endo*-configuration (see Fig. 7).

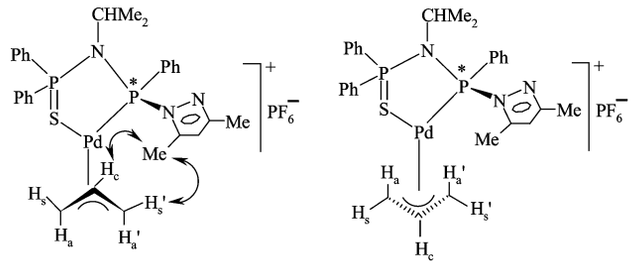

endo-; (**11a**) *exo*-; (**11b**)

Fig. 7 The two Pd(II)–allyl diastereomers of diphosphazane monosulfide, $[Pd(\eta^3\text{-}C_3H_5)\{\kappa^2\text{-}Ph_2P(S)N(CHMe_2)PPh(N_2C_3HMe_2$-3,5)$\}](PF_6)$ (**11**), observed in solution. Selective NOE contacts reveal that in the *endo*-isomer, the central allyl proton and pyrazole-3-Me protons are close to each other whereas for the *exo*-isomer, such an NOE contact with the central allyl proton is absent.

The absence of such an interaction in the minor isomer (**11b**) indicates that this isomer has an *exo*-configuration.

The $^{31}P\{^1H\}$ NMR spectrum of the 1,3-dimethyl allyl complex **12** shows three pairs of doublets in the ratio 6 : 4 : 1 indicating the presence of three isomers (**12a**–**c**) in solution. The ^1H NMR spectrum shows three different sets of allyl protons each consisting of three resonances. All the proton resonances are unambiguously assigned by recourse to standard ^1H–^1H 2D homo correlation techniques. The ^{13}C NMR spectrum is assigned with the help of 2D ^1H–^{13}C heteronuclear correlation spectrum. The doublet pattern observed for one of the terminal allylic carbon resonances clearly point to P,S-coordination. The signal arising from the third isomer **12c** could not be seen in the ^{13}C NMR spectrum owing to its relative low abundance. However, the $^{31}P\{^1H\}$ and ^1H chemical shifts and $^2J(P,P)$ coupling constant values for **12c** are similar to those of **12a** and **12b**. Hence, **12c** must be structurally close to **12a** and **12b**. The ^1H–^1H COSY spectrum indicates the presence of two *anti* allyl protons for isomers **12a** and **12b** *i.e.* the methyl groups are in the *syn*/*syn*-arrangements (see Fig. 8). This arrangement is supported by the expected NOE interactions between the central allyl proton and two allyl methyl groups for

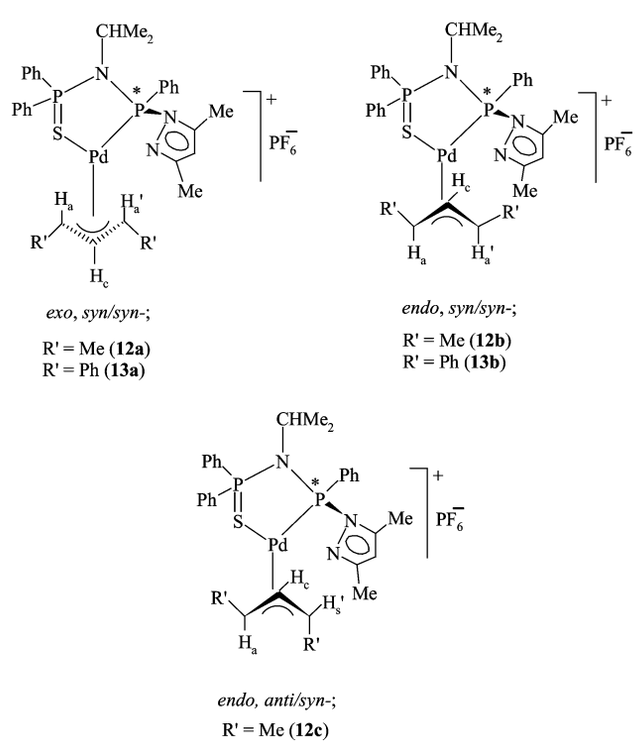

exo, *syn*/*syn*-;
R' = Me (**12a**)
R' = Ph (**13a**)

endo, *syn*/*syn*-;
R' = Me (**12b**)
R' = Ph (**13b**)

endo, *anti*/*syn*-;
R' = Me (**12c**)

Fig. 8 The three isomers observed in solution for 1,3-disubstituted allyl palladium complexes, $[Pd(\eta^3\text{-}1,3\text{-}R'_2\text{-}C_3H_3)\{\kappa^2\text{-}Ph_2P(S)N(CHMe_2)\text{-}PPh(N_2C_3HMe_2$-3,5)$\}](PF_6)$ [R′ = Me (**12**); R′ = Ph (**13**)].

the isomers, **12a** and **12b**. It is difficult to determine the allylic arrangement for **12c** from the ^{1}H–^{1}H COSY spectrum because the resonances of both the allyl protons appear at the same position (4.75 ppm). However, a careful analysis of the ^{1}H–^{1}H NOESY spectrum reveals that **12c** is the *anti*/*syn*-isomer, because only the methyl proton resonances at 1.99 ppm show an NOE interaction to the central allyl proton, H_c and the other methyl proton resonances at 0.31 ppm do not show any NOE interaction with H_c as would be expected for the *anti*/*syn*-isomer in which the *anti*-allyl methyl group is located *trans* to the sulfur atom (see Fig. 8). In contrast to the situation for complex **11**, the major isomer (**12a**) observed in solution for complex **12**, possesses the *exo*-configuration. This is revealed by the NOE interaction between the 5-CH_3 protons of the pyrazole ring and the *anti* allyl proton *trans* to the sulfur centre, H_a'; the absence of such an interaction with the H_c proton also supports the *exo*-configuration for isomer **12a**. The isomers **12b** and **12c** exhibit NOE interaction between the central allyl proton to the respective 5-CH_3 group of the pyrazole ring which is indicative of their *endo*-configuration.

The 1,3-diphenyl allyl complex **13** exists as two isomers **13a** and **13b** in solution (in a 1 : 1.3 ratio) as revealed by its ^{31}P{^{1}H} NMR spectrum. NMR studies on these isomers show that they have the *syn*/*syn*- allylic arrangement. An NOE interaction between 5-CH_3 group of pyrazole ring and central allyl proton establishes that **13a** has the *exo*-configuration whereas **13b** has the *endo*-configuration (Fig. 8).

From a solution of **12** containing three isomers, the major isomer **12a** is isolated as colourless crystals. The structure of **12a** has been determined by X-ray diffraction. An ORTEP view of the molecule is shown in Fig. 9. The X-ray structure shows P,S-coordination with a distorted 'PdC_2PS' core. The Pd–C and Pd–S bond distances (Table 3) are in the expected range observed for Pd(II) allyl compounds with P,S-chelate ligands.[6b] The 5-CH_3 group of the pyrazole and central allyl carbon lie at the opposite side of the coordination plane formed by P(1)–Pd(1)–S(1) revealing the *exo*, *syn*/*syn*-configuration in the solid state.

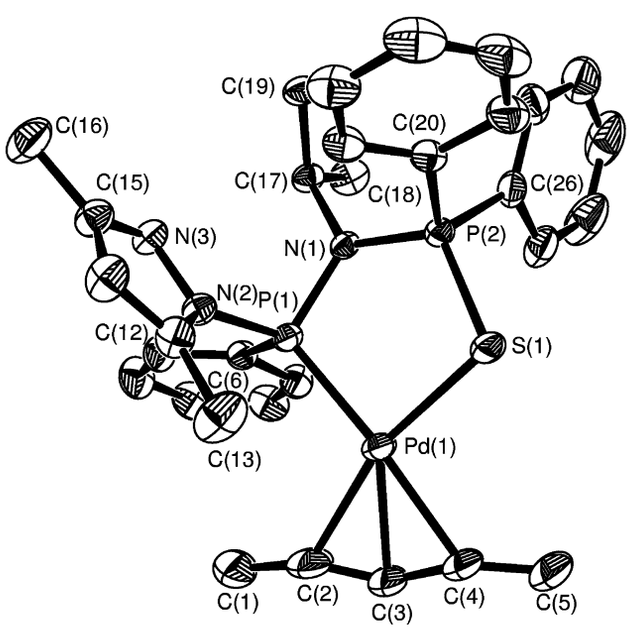

Fig. 9 A view of the molecular structure of **12a** showing the *exo*, *syn*/*syn*-configuration (the hydrogen atoms and the hexafluorophosphate anion are not shown).

Stereodynamic behaviour of allyl complexes 11–13 in solution

The phase sensitive 2D ^{1}H–^{1}H NOESY and ROESY spectra of complex **11** in $CDCl_3$ at 298 K shed light on the intimate nature of the dynamic processes occurring in solution. From the selective exchanges observed (see ESI †), the major exchange pathway is found to be the *cis–trans* isomerisation. Apart from this, a second isomerisation is also observed *via syn–anti* exchange. The *syn–anti* isomerisation is observed only at the allyl terminus *trans* to the sulfur atom, suggesting that the opening of the η^3-allyl ligand to η^1-bonded intermediate is controlled electronically. Despite the occurrence of these two processes in solution, only two diastereomers are observed as the allyl group is unsubstituted. (Such a result is also observed in the case of P,N-coordinated unsubstituted allyl complex **5**.)

The dynamic behaviour of the complexes **12** and **13** has been studied by the phase sensitive ^{1}H–^{1}H NOESY and ROESY spectra in $CDCl_3$ at 298 K. No exchange is observed at 298 K between the isomers **13a** and **13b**. On the other hand, the crystals of **12a** on dissolution in $CDCl_3$ transform into the other two minor isomers **12b** and **12c**. The isomer **12c** does not show any observable exchange. An analysis of the observed exchange cross-peaks between **12a** and **12b** shows that the exchange occurs by a *cis–trans* isomerisation process. A possible mechanism is shown in Scheme 8. The presence of the *anti*/*syn*-isomer (**12c**) indicates that the isomerisation involves initial selective opening of the η^3-allyl group at the allylic carbon *trans* to the coordinated phosphorus atom to generate an η^1-bonded intermediate. This type of selective opening can account for the absence of any *syn*/*anti*-isomer (*i.e.* the *anti* allyl methyl group is located *trans* to the coordinated phosphorus centre) and is well known for P,S-ligands.[27] The ^{1}H–^{1}H NOESY spectrum (see ESI †) shows NOE cross-peaks between the isomers **12a** and **12b**. These intermolecular NOE interactions arise as a result of a fast exchange process in solution. The rapid dynamic process is most probably related to the possibility that the free nitrogen on the pyrazole ring can interact with the palladium centre in the η^1-bonded intermediate. This internal coordination of the pyrazole nitrogen stabilises the η^1-bonded intermediates (**B** and **C** in Scheme 8) and thereby can accelerate the *cis–trans* isomerisation process. It is well known that catalytic amounts of anions such as chloride or fluoride or polar solvents like DMSO or acetonitrile, which can coordinatively interact with palladium centre in the η^1-bonded intermediate, can accelerate the dynamic process.[5e,35] The formation of **12c** can also be rationalised by considering a rotation around C(sp^3)–C(sp^2) bond starting from **12a** *via* the intermediate **B** (see Scheme 8).

Variable temperature NMR studies and activation barriers ($\Delta G^{\neq}$)

In order to determine the activation barriers for the exchange process in some of the above complexes, we have carried out variable temperature ^{1}H NMR studies in DMSO-d_6 at 298–373 K. The coalescence temperatures and the corresponding $\Delta G^{\neq}$[36] values are listed in Table 4. The data show that the change of the substituent on the nitrogen from $CHMe_2$ to CHMePh of the diphosphazane ligand backbone increases the activation barrier of the isomerisation process as observed for the unsubstituted allyl complexes **4** and **5** (see entries 1 and 2) bearing $Ph_2PN(CHMe_2)PPh(N_2C_3HMe_2$-3,5) and $Ph_2PN((S)$*-$CHMePh)PPh(N_2C_3HMe_2$-3,5) ligands, respectively. The incorporation of Ph or Me substituents at the 1,3-allylic positions increases the free energy of activation for the exchange process as compared to the unsubstituted allyl analogs (see entries 1 and 4, entries 2 and 3). The activation barrier for the allyl isomers bearing P,S-ligand is less as compared to the allyl isomers of P,N-ligand (see entries 3, 5 and 6). The activation barrier for *cis–trans* isomerisation process is slightly less than that for the *syn–anti* isomerisation process when the ligand and the allyl moieties are the same (see entries 5 and 6).

Trends in ^{31}P chemical shifts

The ^{31}P{^{1}H} resonances are assigned on the basis of the $\Delta\delta$ [$\Delta\delta = \delta$(complex) $-$ δ(free ligand)] and sensitivity of the chemical shifts upon substitution on the allyl moiety (see Table

Table 4 Variable temperature ^{1}H NMR data[a] and calculated free energy of activation for η^3-allyl palladium complexes of diphosphazane ligands

Entry	Interchanging isomers	$\Delta\nu$/Hz	Coalescence temperature/K	$\Delta G^{\neq}$/kJ mol^{-1}[b]	The protons for which coalescence observed
(1)	**4a** and **4b**	66.0	313	63.7	–N(CHMe$_2$) methyl protons
(2)	**5a** and **5b**	11.6	318	69.4	–N(*CHMePh) methyl protons
(3)	**7a** and **7b**	30.8	363	76.7	Allyl methyl protons *trans* to the coordinated phosphorus centre
(4)	**8b** and **8c**	17.8	368	79.5	–N(CHMe$_2$) methyl protons
(5)	**12a** and **12b**	44.4	318	65.9	–N(CHMe$_2$) methyl protons
(6)	**12a** and **12c**	25.4	324	68.7	–N(CHMe$_2$) methyl protons

[a] DMSO-d$_6$ was used as solvent. [b] Calculated according to the Shanan-Atidi and Bar-Eli method.[36] The estimated error in the calculated free energies of activation is ± 1 kJ mol^{-1}. $\Delta\nu$ = frequency separation in the slow exchange limit.

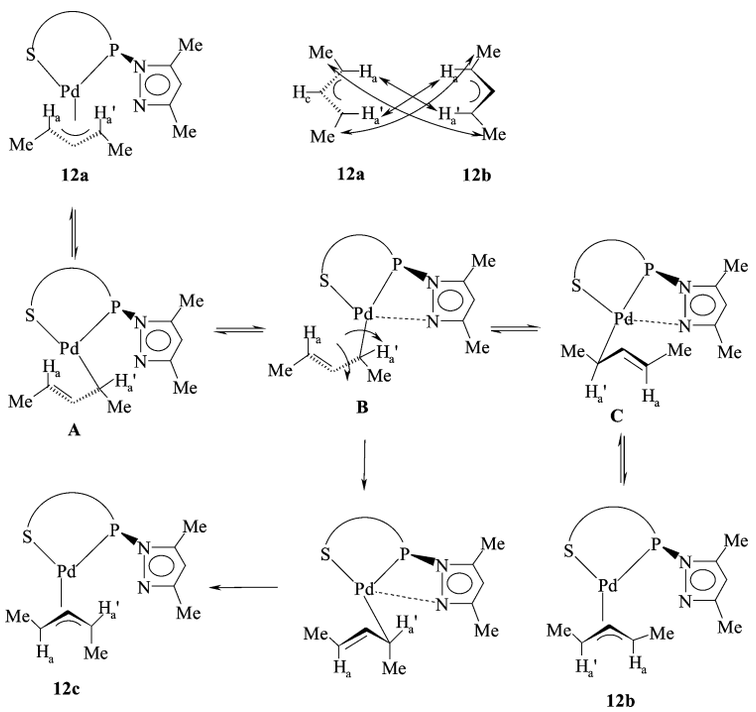

Scheme 8

5). The chemical shift of one of the phosphorus nuclei for all the palladium allyl complexes except for the P,P-coordinated complexes (**8b** and **8c**) lies in the range 70–74 ppm with $\Delta\delta$ being only 0.5–6 ppm. The constancy in the magnitude of chemical shifts on changing the allyl part and the low $\Delta\delta$ value suggest that this chemical shift can be assigned to the non-coordinated phosphorus. On the other hand, the chemical shift of the other phosphorus nucleus shows a greater range of variation (75–83 ppm). This phosphorus chemical shift lies very much downfield as compared to that of the free ligand and the magnitude of $\Delta\delta$ is in the range 31–36 ppm. Hence this chemical shift is assigned to the –PPh$_2$ phosphorus. For the P,P-coordinated complexes (**8b** and **8c**), the –PPh$_2$ and the –PPh(N$_2$C$_3$HMe$_2$-3,5) chemical shifts are assigned the values 62–63 and 69–73 ppm, respectively, based on the observed chemical shifts for 1,3-diphenyl palladium allyl complex of the ligand Ph$_2$PN(CHMe$_2$)PPh$_2$ which features P,P-coordination.[37] For the P,S-coordinated complexes (**11**–**13**), the –P(S)Ph$_2$ and the –PPh(N$_2$C$_3$HMe$_2$-3,5) chemical shifts are assigned the values 73–77 and 91–93 ppm, respectively, based on the the magnitude of $\Delta\delta$ and chemical shifts observed for palladium allyl complexes of the ligands, Ph$_2$P(S)N(CHMe$_2$)PPh$_2$ and Ph$_2$P(S)N(CHMe$_2$)P(S)Ph$_2$.[37] The ^2J(P,P) values for P,N-coordinated complexes of **1** and **2** lie in the range 28–30 Hz whereas ^2J(P,P) values for P,P-coordinated allyl complexes (**8b** and **8c**) are observed in the range of ~110 Hz. The ^2J(P,P) values for the P,S-coordinated complexes of 3 are in the range 87–97 Hz.

Catalytic studies

We tested the catalytic activity of the two diphosphazane ligands (**1** and (*SR*)-**2**) in allylic alkylation reaction of the model substrate, (*rac*)-1,3-diphenyl-2-propenyl acetate (I) (Scheme 9) using dimethyl malonate as the nucleophile.[34] Catalytic precursors are generated *in situ* from [Pd(η^3-C$_3$H$_5$)-(μ-Cl)]$_2$ (1 mol%) and the appropriate ligands (2.5 mol%). The reaction is found to be complete within 24 h as shown by the ^{1}H NMR spectrum of the reaction mixture. However, only low levels of enantiomeric excess (<30%) is observed in these reactions (see Experimental).

The palladium catalysed allylic alkylation with (*E*)-3-phenyl-2-propenyl acetate (III) is investigated to study the regio-selectivity of these systems (Scheme 10). The use of an unsymmetrical substrate, such as III in allylic alkylation would afford a mixture of linear and branched regio-isomers IV and V depending on the nucleophilic attack at one or the other terminal allyl carbon centres. The ^{1}H NMR spectrum of the reaction mixture shows complete conversion of the substrate in 24 h at 298 K and the ratio of linear and branched isomer is *ca.* 70 : 30 indicating that nucleophilic addition is more favoured at the unsubstituted terminal carbon.

Conclusions

The diphosphazane ligands **1**–**3** bearing a stereogenic phosphorus centre exhibit diverse palladium allyl chemistry

Table 5 The $^{31}P\{^{1}H\}$ NMR data[a] for the η^3-allyl palladium complexes **4**–**13**

Complex	–PPh($N_2C_3HMe_2$-3,5) (δ_A)[b]	$\Delta\delta_A$	–P(E)Ph_2 (δ_x)[b]	$\Delta\delta_x$
4a	72.5 d (30.0)	0.6	75.6 d	31.7
4b	72.5[c]	0.6	75.3 d	31.4
5a	72.7 d (28.4)	3.9	77.7 d	30.4
5b	73.0 d (29.0)	4.2	78.4 d	31.1
6a	71.6 d (28.3)	−0.3	79.5 d	35.6
6b	71.3 d (30.2)	−0.6	76.9 d	33.0
6c	71.8 d (29.1)	−0.1	75.4 d	31.5
6d	70.1 d (27.5)	−1.8	78.3 d	34.4
7a	72.7 d (28.9)	3.9	82.3 d	35.0
7b	73.7 d (27.8)	4.9	81.2 d	33.9
7c	73.8 d (28.2)	5.0	78.3 d	31.0
7d	73.0 d (29.4)	4.2	83.4 d	36.1
8a	70.9 d (30.3)	−1.0	80.2 d	36.3
8b	73.1 d (114.3)	1.2	62.4 d	18.5
8c	69.0 d (109.1)	−2.9	63.1 d	19.2
9	70.8 d (28.8)	2.0	81.3 d	34.0
10	72.5 d (28.7)	6.3	81.8 d	32.9
11a	91.1 d (95.3)	20.6	77.1 d	11.8
11b	92.0 d (92.4)	21.5	76.6 d	11.3
12a	92.8 d (91.9)	22.3	74.4 d	9.1
12b	93.0 d (96.8)	22.5	75.8 d	10.5
12c	93.3 d (91.2)	22.8	75.5 d	10.2
13a	91.4 d (92.3)	20.9	74.0 d	8.7
13b	93.1 d (87.2)	22.6	73.5 d	8.2

[a] The $^{31}P\{^{1}H\}$ NMR spectra were recorded in $CDCl_3$ at 298 K except for **6** in which case a 1 : 1 mixture of $CDCl_3$ and CH_2Cl_2 was used. The ^{31}P–^{31}P coupling constants are given in parentheses. $\Delta\delta = \delta$(complex) − δ(free ligand). [b] d: doublet. [c] Overlapped by a signal arising from the –PPh-($N_2C_3HMe_2$-3,5) phosphorus of isomer **4a**.

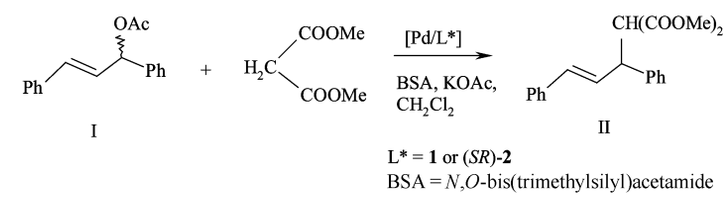

Scheme 9

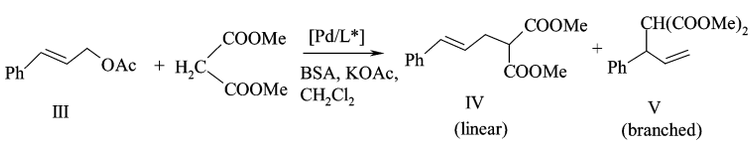

Scheme 10

including various fluxional processes in solution. The ligands **1** and **2** prefer P,N-coordination rather than the usually observed P,P-coordination as the former mode of coordination electronically stabilises the palladium allyl bonding besides leading to the formation of a stable six-membered chelate ring. The usual P,P-coordination is observed only in the case of 1,3-diphenyl allyl system (complex **8**) probably because of the higher electron releasing ability of two phenyl groups thus obviating the necessity of having the σ-donor pyrazole nitrogen to stabilise the metal allyl bonding. On the other hand, the diphosphazane monosulfide ligand, $Ph_2P(S)N(CHMe_2)PPh$-($N_2C_3HMe_2$-3,5) (**3**) displays P,S-coordination. The P,S-coordination is preferred owing to the formation of a stable five-membered ring around the palladium centre. Thus the choice of a particular coordination mode (P,N- or P,P- or P,S-) for the ligands **1**–**3** is the result of combined effect of chelate ring size around the palladium centre as well as electronic nature of the allyl moiety.

The allyl palladium complexes formed by these ligands (**1**–**3**) exist as several isomers in solution. However, the solid state structures reveal the presence of only one isomer. In the solid state, the P,N-coordinated complexes (**5a**, **7a** and **8a**) show the *endo* configuration for the allyl moity whereas the solid state structure of P,S-coordinated complex (**12a**) reveals *exo*-configuration. The isomer observed in the solid state undergoes slow isomerisation to produce a mixture of several isomers in solution. The exchange pathway involves two well-known processes, namely *cis–trans* isomerisation and *syn–anti* exchange through a common σ-bonded intermediate. The σ-bonded intermediate is generated by the opening of the η^3-allyl moiety at the *trans* position with respect to the greater π-acceptor phosphorus centre and is thus subject to electronic control. The activation barriers for exchange processes among various allyl isomers bearing the P,S-ligand is less than that observed for the allyl isomers formed by the P,N-ligands.

Acknowledgements

We thank the Department of Science and Technology (DST), New Delhi, India for financial support.

References

1 (*a*) B. M. Trost and T. R. Verhoeven, in *Comprehensive Organometallic Chemistry*, ed. G. Wilkinson, F. G. A. Stone and E. W. Abel, Pergamon Press, Oxford, 1982, 8, 799; (*b*) P. von Matt

and A. Pfaltz, *Angew. Chem., Int. Ed. Engl.*, 1993, **32**, 566; (*c*) T. Hayashi, in *Catalytic Asymmetric Synthesis*, ed. I. Ojima, VCH Publishers, New York, 1993, 325; and references cited therein; (*d*) R. Noyori, *Asymmetric Catalysis in Organic Synthesis*, Wiley, New York, 1994, 82; (*e*) B. M. Trost and D. L. V. Vranken, *Chem. Rev.*, 1996, **96**, 395; (*f*) G. Consiglio and R. M. Waymouth, *Chem. Rev.*, 1989, **89**, 257; (*g*) C. G. Frost, J. Howarth and J. M. J. Williams, *Tetrahedron: Asymmetry*, 1992, **3**, 1089; (*h*) G. Helmchen, *J. Organomet. Chem.*, 1999, **576**, 203.

2 (*a*) P. S. Pregosin and R. Salzmann, *Coord. Chem. Rev.*, 1996, **155**, 35; (*b*) P. S. Pregosin and G. Trabesinger, *J. Chem. Soc., Dalton Trans.*, 1998, 727; (*c*) P. S. Pregosin, H. Rüegger, R. Salzmann, A. Albinati, F. Lianza and R. W. Kunz, *Organometallics*, 1994, **13**, 83; (*d*) J. M. Canal, M. Gómez, F. Jiménez, M. Rocamora, G. Muller, E. Duñach, D. Franco, A. Jiménez and F. H. Cano, *Organometallics*, 2000, **19**, 966; (*e*) A. Gogoll, C. Johansson, A. Axén and H. Grennberg, *Chem. Eur. J.*, 2001, **7**, 396.

3 J. K. Whitesell, *Chem. Rev.*, 1989, **89**, 1581.

4 S. Murray, S. Hartley and F. Hartley, *Chem. Rev.*, 1981, **81**, 365.

5 (*a*) A. Pfaltz, *Acta Chem. Scand. Ser. B*, 1996, **50**, 189 and references cited therein; (*b*) S. Kudis and G. Helmchen, *Angew. Chem., Int. Ed.*, 1998, **37**, 3047; (*c*) G. J. Dawson, C. G. Frost, J. M. J. Williams and S. J. Coote, *Tetrahedron Lett.*, 1993, **34**, 3149; (*d*) G. Helmchen, S. Kudis, P. Sennhenn and H. Steinhagen, *Pure Appl. Chem.*, 1997, **69**, 513 and references cited therein; (*e*) J. M. Brown, D. I. Hulmes and P. J. Guiry, *Tetrahedron*, 1994, **50**, 4493.

6 (*a*) D. A. Evans, K. R. Campos, J. S. Tedrow, F. E. Michael and M. R. Gagné, *J. Org. Chem.*, 1999, **64**, 2994; (*b*) D. A. Evans, K. R. Campos, J. S. Tedrow, F. E. Michael and M. R. Gagné, *J. Am. Chem. Soc.*, 2000, **122**, 7905; (*c*) A. Albinati, P. S. Pregosin and K. Wick, *Organometallics*, 1996, **15**, 2419; (*d*) A. Albinati, J. Eckert, P. S. Pregosin, H. Rüegger, R. Salzmann and C. Stoggel, *Organometallics*, 1997, **16**, 579.

7 (*a*) T. Morimoto, K. Tachibana and K. Achiwa, *Synlett.*, 1997, 783; (*b*) J. C. Anderson, D. S. James and J. P. Mathias, *Tetrahedron: Asymmetry*, 1998, **9**, 753; (*c*) J. V. Allen, J. F. Bower and J. M. J. Williams, *Tetrahedron: Asymmetry*, 1994, **5**, 1895; (*d*) K. Boog-Wick, P. S. Pregosin and G. Trabesinger, *Organometallics*, 1998, **17**, 3254.

8 G. Helmchen and A. Pfaltz, *Acc. Chem. Res.*, 2000, **33**, 336.

9 (*a*) O. Reiser, *Angew. Chem., Int. Ed. Engl.*, 1993, **32**, 547; (*b*) P. B. Mackenzie, J. Whelan and B. Bosnich, *J. Am. Chem. Soc.*, 1985, **107**, 2046.

10 A. Togni, U. Burckhardt, V. Gramlich, P. S. Pregosin and R. Salzmann, *J. Am. Chem. Soc.*, 1996, **118**, 1031.

11 (*a*) M. Ganesan, S. S. Krishnamurthy and M. Nethaji, *J. Organomet. Chem.*, 1998, **570**, 247; (*b*) R. P. K. Babu, K. Aparna, S. S. Krishnamurthy and M. Nethaji, *Phosphorus, Sulfur Silicon Relat. Elem.*, 1995, **103**, 39; (*c*) R. P. K. Babu, S. S. Krishnamurthy and M. Nethaji, *Organometallics*, 1995, **14**, 2047; (*d*) R. P. K. Babu, S. S. Krishnamurthy and M. Nethaji, *Polyhedron*, 1996, **15**, 2689; (*e*) R. P. K. Babu, S. S. Krishnamurthy and M. Nethaji, *J. Organomet. Chem.*, 1993, **454**, 157; (*f*) K. Raghuraman, S. S. Krishnamurthy and M. Nethaji, *J. Chem. Soc., Dalton Trans.*, 2002, 4289; (*g*) Part 16. K. Raghuraman, S. S. Krishnamurthy and M. Nethaji, *J. Organomet. Chem.*, in press.

12 For reviews on this topic see: (*a*) M. S. Balakrishna, V. S. Reddy, S. S. Krishnamurthy, J. F. Nixon and J. C. T. R. Burckett St Laurent, *Coord. Chem. Rev.*, 1994, **129**, 1; (*b*) M. Witt and H. W. Roesky, *Chem. Rev.*, 1994, **94**, 1163; (*c*) P. Bhattacharyya and J. D. Woollins, *Polyhedron*, 1995, **14**, 3367.

13 S. K. Mandal, G. A. Nagana Gowda, S. S. Krishnamurthy, C. Zheng, S. Li and N. S. Hosmane, *Eur. J. Inorg. Chem.*, 2002, 2047.

14 D. D. Perrin, W. L. F. Armarego and D. R. Perrin, *Purification of Laboratory Chemicals*, Pergamon Press, Oxford, 3rd edn., 1988.

15 Y. Tatsuno, T. Yshida and S. Otsuka, *Inorg. Synth.*, 1990, **28**, 342.

16 P. R. Auburn, P. B. McKenzie and B. Bosnich, *J. Am. Chem. Soc.*, 1985, **107**, 2033.

17 P. von Matt, G. C. Lloyd-Jones, A. B. E. Minidis, A. Pfaltz, L. Macko, M. Neuburger, H. Rüegger and P. S. Pregosin, *Helv. Chim. Acta*, 1995, **78**, 265.

18 R. P. K. Babu, S. S. Krishnamurthy and M. Nethaji, *Tetrahedron: Asymmetry*, 1995, **6**, 427.

19 G. M. Sheldrick, SHELXS86, Program for solution of crystal structures, University of Göttingen, Germany, 1986.

20 G. M. Sheldrick, SHELXS-97, Program for solution of crystal structures, University of Göttingen, Germany, 1997.

21 H. D. Flack, *Acta Crystallogr.*, 1983, **A39**, 876.

22 A. Togni, *Tetrahedron: Asymmetry*, 1991, **2**, 683.

23 (*a*) N. Baltzer, L. Macko, S. Schaffner and M. Zehnder, *Helv. Chim. Acta*, 1996, **79**, 803; (*b*) R. Fernández-Galán, F. A. Jalón, B. R. Manzano, J. R. Fuente, M. Vrahami, B. Jedlicka, W. Weissensteiner and G. Jogl, *Organometallics*, 1997, **16**, 3758; (*c*) J. Powell and B. L. Shaw, *J. Chem. Soc. A*, 1967, 1839; (*d*) B. Åkermark, B. Krakenberger, S. Hansson and A. Vitagliano, *Organometallics*, 1987, **6**, 620.

24 (*a*) S. Sakaki, K. Takeuchi and M. Sugimoto, *Organometallics*, 1997, **16**, 2995; (*b*) C. Carfagna, R. Galarini, K. Linn, J. A. Lòpez, C. Mealli and A. Musco, *Organometallics*, 1993, **12**, 3019; (*c*) H. Fujimoto and T. Suzuki, *Int. J. Quantum Chem.*, 1999, **74**, 735.

25 J. W. Faller, M. E. Thomson and M. Mattina, *J. Am. Chem. Soc.*, 1971, **93**, 2642.

26 C. Breutel, P. S. Pregosin, R. Salzmann and A. Togni, *J. Am. Chem. Soc.*, 1994, **116**, 4067.

27 J. Hermann, P. S. Pregosin, R. Salzmann and A. Albinati, *Organometallics*, 1995, **14**, 3311.

28 T. Hosokawa, Y. Wakabayashi, K. Hosokawa, T. Tsuji and S.-I. Murahashi, *Chem. Commun.*, 1996, 859.

29 J. Sprinz, M. Keifer, G. Helmchen, M. Reggelin, G. Huttner, O. Walter and L. Zsolnai, *Tetrahedron Lett.*, 1994, **35**, 1523.

30 S. Lanza, G. Bruno, F. Nicolò, A. Rotondo, R. Scopelliti and E. Rondo, *Organometallics*, 2000, **19**, 2462.

31 B. Crociani, S. Antonaroli, G. Bandoli, L. Canovese, F. Visentin and P. Uguagliati, *Organometallics*, 1999, **18**, 1137.

32 U. Burckhardt, V. Gramlich, P. Hoffmann, R. Nesper, P. S. Pregosin, R. Salzmann and A. Togni, *Organometallics*, 1996, **15**, 3496.

33 For a review, see *e.g.*: T. G. Appleton, H. C. Clark and L. Manzer, *Coord. Chem. Rev.*, 1973, **10**, 335.

34 B. M. Trost and D. J. Murphy, *Organometallics*, 1985, **4**, 1143.

35 (*a*) S. Hansson, P-O. Norrby, M. P. T. Sjögren, B. Åkermark, M. E. Cucciolito, F. Giordano and A. Vittagliano, *Organometallics*, 1993, **12**, 4940; (*b*) U. Burckhardt, M. Baumann, G. Trabesinger, V. Gramlich and A. Togni, *Organometallics*, 1997, **16**, 5252.

36 J. Sandström, *Dynamic NMR Spectroscopy*, Academic Press, London, 1982.

37 S. K. Mandal, G. A. N. Gowda, S. S. Krishnamurthy, C. Zheng, S. Li and N. S. Hosmane, *J. Organomet. Chem., in press.*